OR. 1214

SAND-79-1424
Unlimited Release

TTC-0018

POSTMORTEM METALLURGICAL EXAMINATION OF A FIRE-EXPOSED SPENT FUEL SHIPPING CASK

H. J. Rack, H. R. Yoshimura

F 2900-Q(3-80)

UC-71

TTC-0018
SAND-79-1424
Unlimited Release
Printed April 1980

POSTMORTEM METALLURGICAL EXAMINATION OF A FIRE-EXPOSED SPENT FUEL SHIPPING CASK

H. J. Rack
Mechanical Metallurgy Division 5835

and

H. R. Yoshimura
Transportation Systems Technology Division 4552
Sandia Laboratories, Albuquerque, New Mexico 87185

ABSTRACT

A postmortem examination of a large fire-exposed rail-transported spent fuel shipping container has revealed the presence of two macrofissures in the outer cask shell. The first, a part-thru crack located within the seam weld fusion zone of the outer cask shell, was typical of hot cracks that may be found in stainless steel weldments. The second, located within the stainless steel base metal, apparently originated at microcracks formed during the welding of a copper-stainless steel dissimilar metal joint. The latter microcrack then propagated during the fire-test, ultimately penetrating the outer shell of the cask.

TABLE OF CONTENTS

FIGURES

TABLES

INTRODUCTION

During January 1978, a 67 metric ton spent fuel shipping container was exposed to a JP-4 fueled fire. This test was intended to simulate a severe, but highly improbable, fire-associated accident condition which might be encountered by a shipping cask. The shipping container used in this test was originally constructed in 1962. It was a double-walled, lead-shielded cylindrical vessel 3.96 m long and 1.5 m in diameter. The inner cask liner had been fabricated from two pieces of 9.4 mm thick 304 stainless steel with one girth and one seam weld. The outer shell was manufactured from two pieces of 34.8 mm thick 304 stainless steel while the top and bottom of the vessel were ACI type CF8 stainless steel castings. Initially, the cask utilized an auxiliary water cooling system consisting of 3.05 mm thick copper channels longitudinally welded to the outside of the cask inner cavity wall. These channels were subsequently replaced by 304 stainless steel channels when it was discovered that the original copper channels had been dissolved during the first lead pour. Additionally, copper fins were longitudinally welded to the inside of the outer shell to enhance the thermal path between the lead shielding and the outer shell.

Prior to the fire test, the cask/railcar system was subjected to a 131 km/h impact into a massive concrete barrier. As predicted by the analytical modeling and scale model testing performed prior to the full scale crash test, the cask survived the impact without failure. The cask's structural shell remained elastic during impact, and only minor cooling fin damage occurred. Post-crash test inspection revealed that the cask outer shell had not been penetrated and that the cask had retained its internal cavity pressure.

After the crash test, the cask and railcar were moved to the fire site and placed over a specially constructed fuel pool. The railcar was supported by concrete pedestals located centrally in the pool, with wheel trucks under one end of the car to maintain its post impact orientation. This positioning subjected the cask to maximum flame temperatures.

Flame temperatures during the fire test ranged from 1250 to 1475 K with the container showing no signs of degradation for at least 90 minutes. At about 100

minutes into the test, a white cloud of smoke, presumably lead oxide, was observed. The fuel supply was stopped and the fire self-extinguished at about 125 minutes. Because of the weakened condition of the concrete and metal supports and the railcar frame, the railcar toppled on its side at this point--severing all instrumentation connections. Internal thermocouples on the cask indicated however that complete lead melt had occurred prior to toppling.

This report presents the results of a postmortem examination of this fire-exposed spent fuel shipping cask.

RESULTS AND DISCUSSION

Figure 1 shows a side view of the shipping cask after the fire exposure. Visual examination indicated that Region A in Figure 1 contained two macrofissures. Both cracks, shown in more detail in Figure 2, had their major direction lying parallel to the longitudinal axis of the cask. Crack no. 1 was located within the seam weld fusion zone region while crack no. 2 lay in the 304 stainless steel base metal. The latter crack also showed indications of lead seepage and gross plastic deformation.

Crack No. 1

This crack was approximately 115 mm long and was located 12 mm from the centerline of the stainless steel seam weld, Figure 3. Examination of the internal surface of the outer shell indicated that the weldment had been fabricated using a backup strip, Figure 4. Chemical analysis of the base metal, fusion zone and backup strip, Table 1, showed that they all met the requirements of 304 stainless steel. The higher chromium content of the weld fusion zone does suggest, however, that 308 filler wire was used in its manufacture.

Observation of the crack surface, Figure 5, showed that crack no. 1 had initiated on the external surface of the outer cask shell and had not completely penetrated the outer shell wall. Figure 5 also shows that the original seam weld had not resulted in full weld penetration. At this inspection point approximately 20 percent of the outer shell thickness had not been joined by the seam welding procedure utilized for the original cask fabrication.

Metallographic sections taken normal to crack no. 1 illustrate the multipass character of the weldment, Figure 6. Further higher magnification examination revealed the presence of numerous internal microcracks. These cracks tended to lie along the austenite-δ ferrite interface, changing direction when traversing from one weld puddle to the next, Figure 7.

Comparison with previous studies of weld cracking in austenitic stainless steels[1] suggests that these internal microcracks, and by implication crack no. 1,

Figure 1. Side view of spent fuel shipping container following fire test.

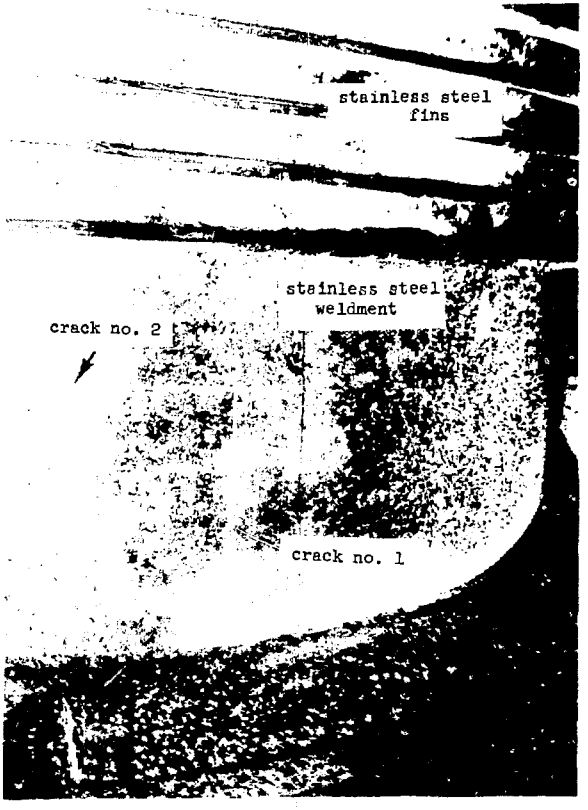

Figure 2. Enlarged view of Region A in Figure 1.

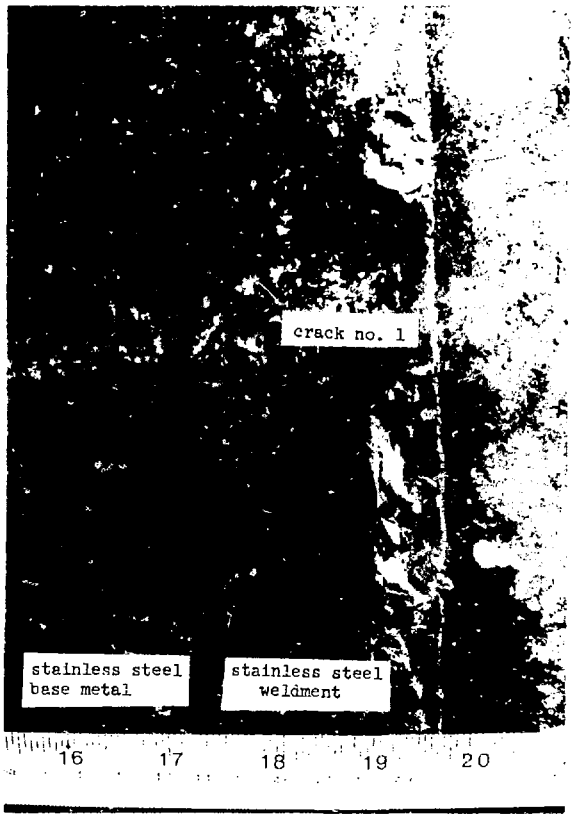

Figure 3. Closeup of crack no. 1.

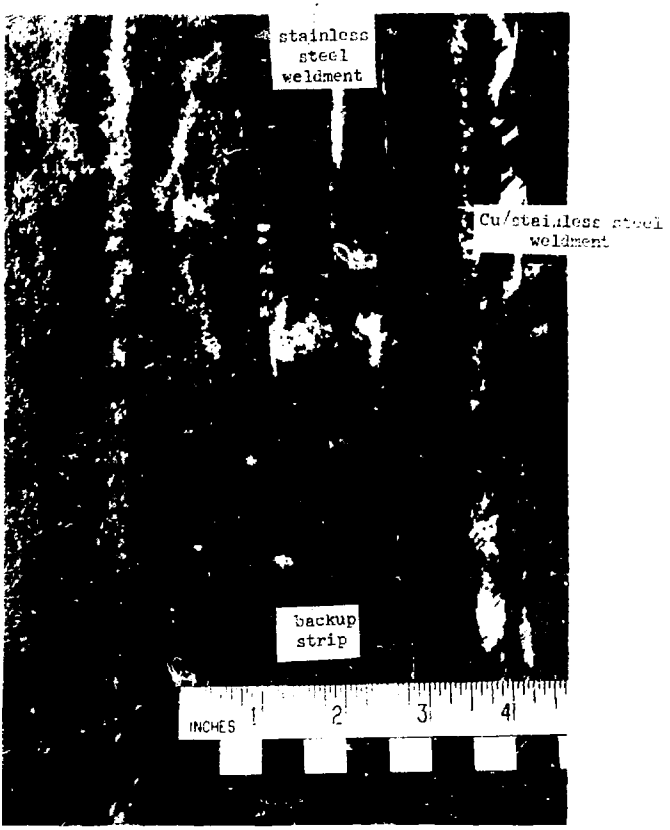

Figure 4. Closeup of outer shell interior surface immediately behind crack no. 1.

Table 1

Chemical Composition of Spent Fuel Shipping Cask Materials

	Element (Weight Percent)								
Part	Cr	Ni	C	Mn	Si	P	S	Mo	Cu
Cask Body	18.3	9.6	0.03	1.51	0.39	0.02	0.01	0.25	0.24
Fusion Zone	19.3	9.9	0.06	1.01	0.47	0.03	0.01	0.11	0.14
Backup Strip	18.0	9.8	0.06	1.1	0.49	0.024	0.01	0.2	0.24

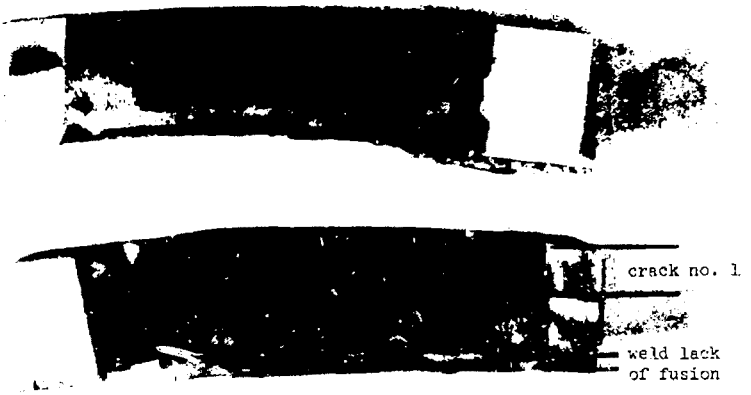

Figure 5. Macroview of crack no. 1.

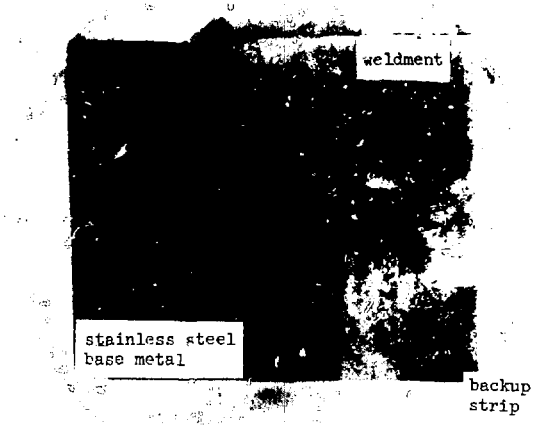

Figure 6. Metallographic section normal to crack no. 1. Magnification: 2X.

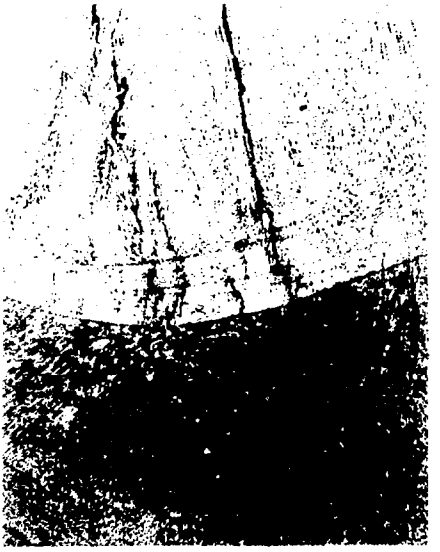

Figure 7. Optical micrograph showing internal cracking in stainless steel weld fusion zone. Magnification: 25X.

are hot cracks. Hot cracking of austenitic stainless steel weldments is generally associated with the presence of a low melting point liquid film at the austenite-ferrite interface. This liquid film reduces the local cohesive strength of the stainless steel weldment. Concurrent stress application then results in crack formation.

Scanning electron microscope observations support the aforementioned hypothesis that crack no. 1 was a hot crack formed in the weld fusion zone during the fire test. Elemental analysis of droplets lying on the fracture surface, e.g., those shown in Figure 8, indicated that they contain substantial amounts of sulfur, probably in the form of complex alloy sulfides. Comparing typical values for alloy sulfide melting points (1250-1475 K)[1] with measured cask temperatures suggests that these sulfides were molten under the present fire test conditions. The further requirement, an applied stress, was apparently supplied by internal pressurization of the fire-exposed spent fuel shipping cask. Indeed internal pressurization within the lead gamma shield cavity was accentuated in the present instance by a manufacturing oversight whereby passage holes from the shield cavity to appropriate expansion volumes originally provided for in the cask design were omitted during cask fabrication.

Crack No. 2

This crack was approximately 70 mm long and was located in the stainless steel base metal, Figure 9. Optical metallography utilizing procedures outlined in ASTM A262-70, Standard Recommended Practices for Detecting Susceptibility to Intergranular Attack in Stainless Steels, Figure 10, and mechanical property evaluation, Table 2, showed that the cask outer shell base metal, after the fire exposure, was in the solution annealed state.

Visual observations of the inside surface of the outer shell immediately behind crack no. 2 confirmed that copper fins had been welded to the outer shell, Figure 11. Further study indicated that many of these copper/stainless steel weldments were cracked. Figures 12 and 13 present two views of such joint cracks. Detailed examination of these cracks showed that they were predominately intergranular, following the stainless steel, austenite, grain boundaries, Figure 14. Microprobe examination, Figure 15, also showed that the cracks contained significant quantities of copper

(a)

(b)

Figure 8. a) Scanning electron micrograph of crack no. 1 fracture surface.

b) Elemental analysis photograph of droplet shown in (a).

Figure 9. Closeup of crack no. 2.

Table 2

Room Temperature Tensile Properties *
of 304 Stainless Steel Cask Outer Shell

Sample Orientation	Yield Strength (MPa)	Ultimate Tensile Strength (MPa)	Percent Total Elongation	Percent Reduction Area
Longitudinal	221	565	80	83
Transverse	217	563	82	76

*Average of duplicate tests, $\dot{\varepsilon} = 5 \times 10^{-3}$ sec^{-1}

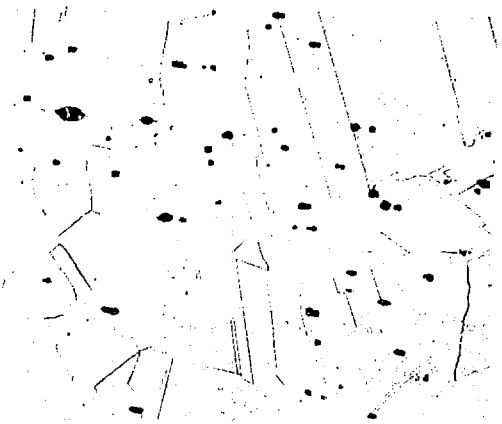

Figure 10. Optical micrograph of 304 stainless steel cask outer shell. Magnification: 250X.

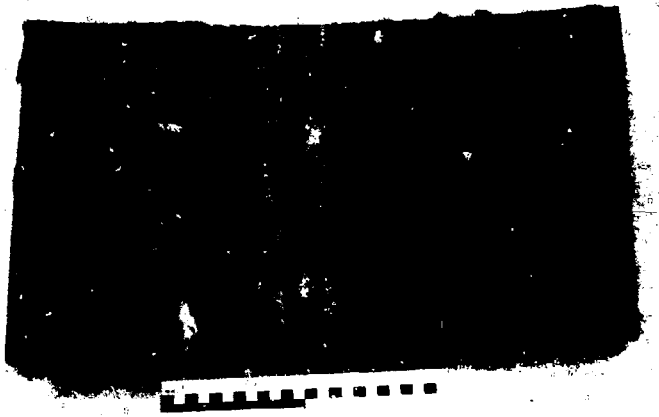

Figure 11. View of interior surface of outer shell showing copper cooling fins joined to shell.

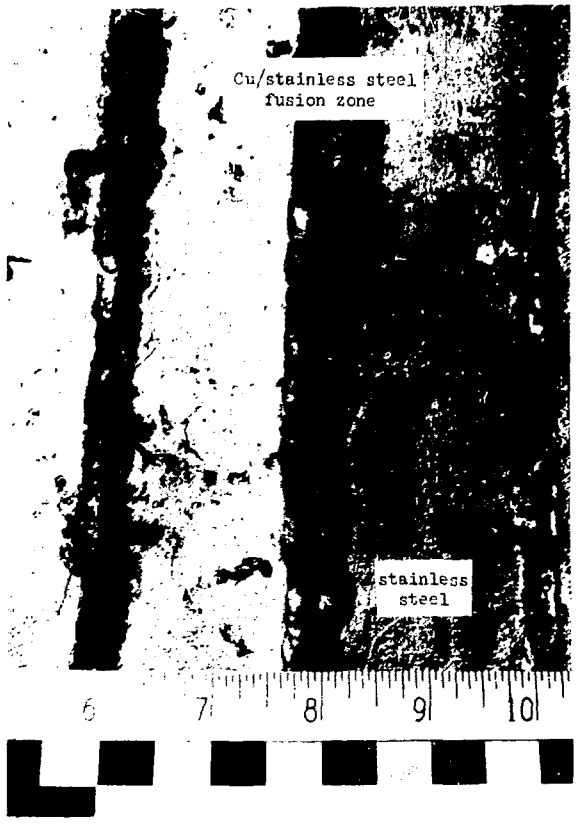

Figure 12. Enlargement of inner surface of outer shell. Arrows indicate copper/stainless steel joint cracks.

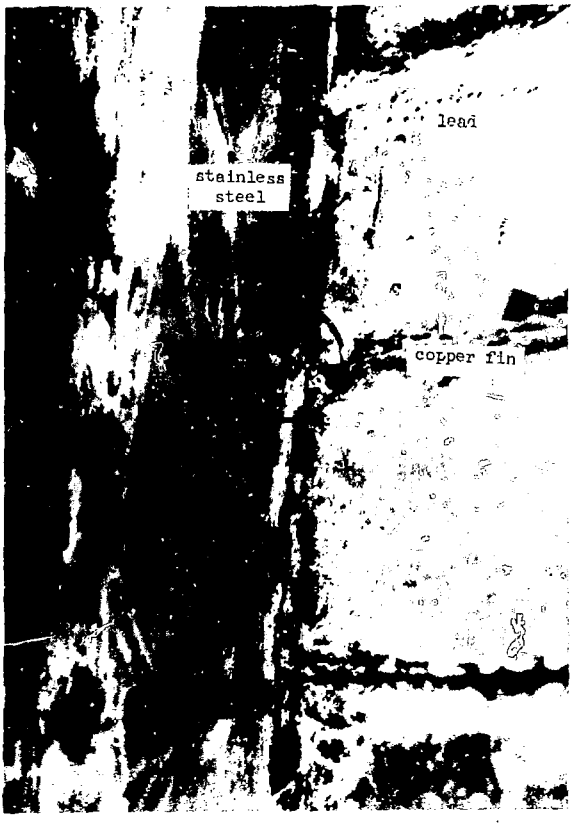

Figure 13. Typical crack observed originating from copper-stainless steel weldment.

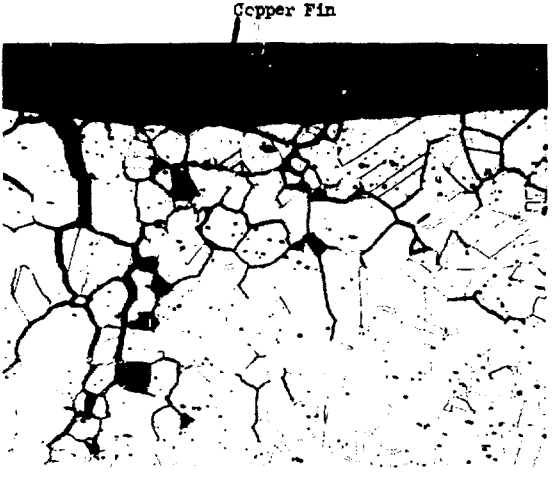

Figure 14. Optical micrograph illustrating intergranular character of cracks in stainless steel. Magnification: 100X.

Figure 15. Identical area elemental distribution photomicrographs of crack in 304 stainless steel. Magnification: 100X.

and lead and lesser amounts of aluminum and silicon. While the elemental enrichment of copper and lead appeared to extend to the crack tip, the aluminum and silicon enrichment appeared to be somewhat more restrictive.

Figure 16 shows a macroscopic view of crack no. 2. Elemental analysis of this fracture surface, Figure 17, showed that copper could be detected to a depth of approximately 17 mm, i.e., ~ 50 percent of the outer cask shell wall thickness.

Numerous investigators[3-7] have shown that a combination of high heat input and direct contact between molten copper and stainless steel will lead to microcracking of the stainless steel during weld fabrication. Generally, successful welding of copper to stainless steel requires that low heat inputs be combined with the use of a nickel filler wire.[8] Microprobe examination of the copper-stainless steel fusion zone indicated that, in this instance, neither of these requirements had been fulfilled. The presence of a high concentration of copper and aluminum in the copper-stainless steel weld fusion zone, Figure 18, suggests that a copper base filler wire had been used to join the copper cooling fins to the cask outer shell. Further analysis of the droplets shown in Figure 18 also indicated that they contained appreciable quantities of iron and chromium. The form of these droplets and their chemistry suggest that they were formed by a high heat input which caused localized melting of the 304 stainless steel during welding.

Consideration of the above observations suggests that crack no. 2 originated from microcracks formed during welding of the copper cooling fins to the stainless steel outer shell. It appears that final crack propagation thru the outer shell wall occurred during the fire-test, the driving force for this crack propagation being supplied by the internal pressurization within the lead gamma shield alluded to previously.

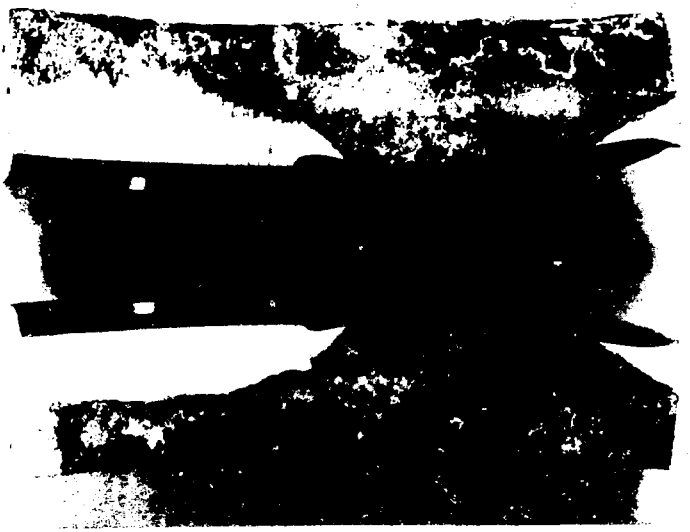

Figure 16. Macroview of crack no. 2.

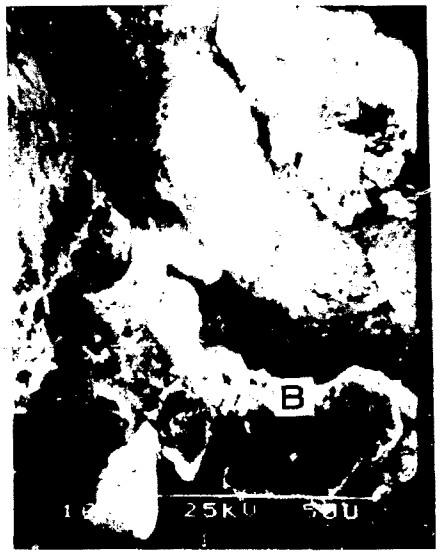

(a)

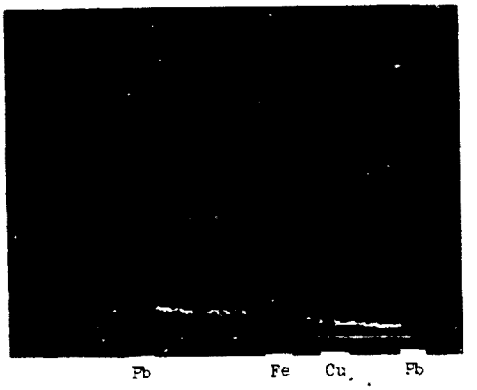

(b)

Figure 17. a) Scanning electron micrograph of crack no. 2 fracture surface.

b) Elemental analysis photograph of Region B near mid-section of crack no. 2.

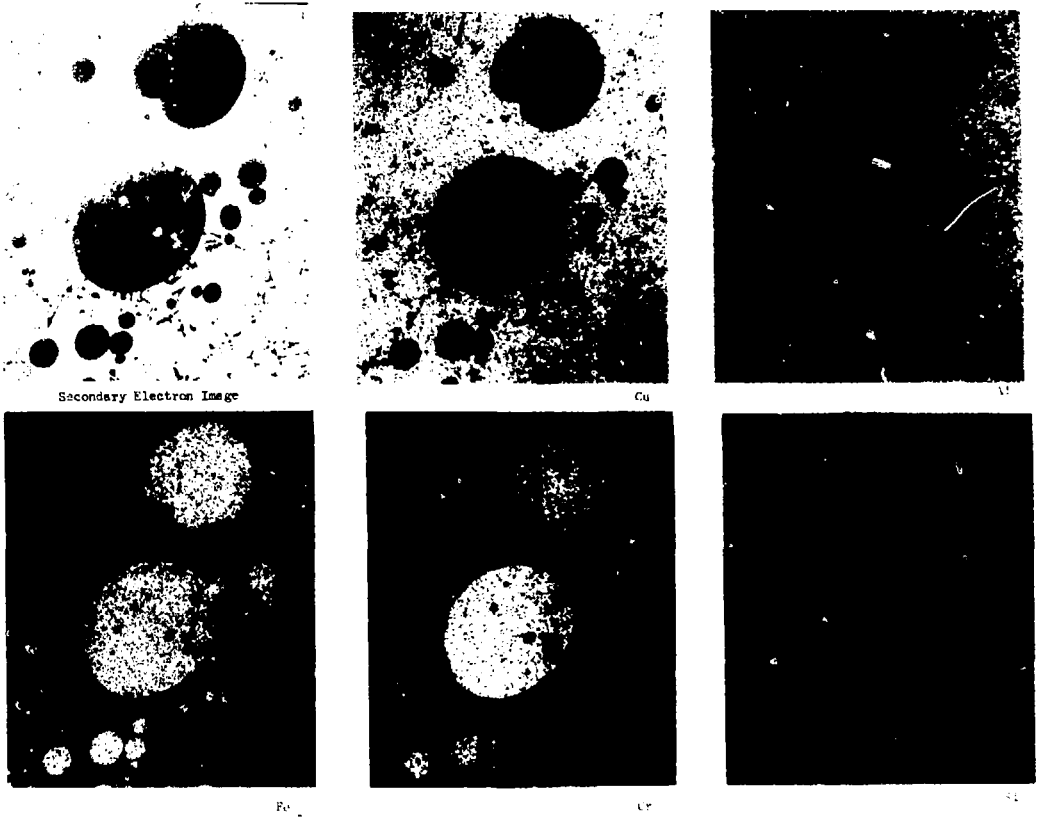

Figure 18. Identical area elemental distribution photomicrographs of copper-stainless steel weld fusion zone. Magnification: 500 X.

SUMMARY AND CONCLUSIONS

Postmortem metallurgical examination of a large rail-transported spent fuel shipping cask which had been exposed to a JP-4 fuel fire revealed the presence of two macrofissures in the outer cask shell. The first, lying within a stainless steel seam weld fusion zone, is believed to be a hot crack which resulted from elevated temperature stressing of the cask. The second crack, located within the stainless steel base metal, appears to originate at a copper-stainless steel dissimilar metal weld joint during manufacture, with final propagation thru the outer cask shell occurring during the fire-exposure. Finally, the present observations suggest that neither macrofissure would have formed if (a) the fire test temperature had not been excessive, that is exceeding the Nuclear Regulatory Commission (1075 K - 30 min.) regulation, (b) appropriate lead expansion volumes had been provided, and (c) appropriate procedures, e.g., a Ni filler wire and low heat input, had been used during welding of the copper fins to the stainless steel outer shell.

ACKNOWLEDGMENTS

The authors wish to acknowledge the assistance of D. R. Stenberg, R. E. Blose, J. Healy and P. Hlava with testing, scanning electron microscopy and microprobe analysis.

REFERENCES

1. T. G. Gooch, "Welding Metallurgy of Stainless Steel," Stainless Steel, Iron and Steel Institute Publication No. 117, Iron and Steel Institute, London, 1969, pp. 77-84.
2. Letter from E. Lusk to H. R. Yoshimura, dated April 19, 1978.
3. V. R. Abramovich, B. P. Alentov and V. I. Parfenov, "An Evaluation of the Effect of Molten Copper and Its Alloys on the Mechanical Properties of Steel," Avt. Svarka, 12, 17 (1977).
4. N. A. Bareskov, "Cracking Susceptibility of Stainless Steels in Brazing with Copper," Svar. Proiz., 11, 38 (1975).
5. W. F. Savage, E. F. Nippes and M. C. Mushala, "Liquid-Metal Embrittlement of the Heat-Affected Zone by Copper Contamination," Welding Jn. Research Supp. 57, 237 (1978).
6. W. F. Savage, E. F. Nippes and M. C. Mushala, "Copper-Contamination Cracking in the Weld Heat-Affected Zone," Welding Jn. Research Supp. 57, 145 (1978).
7. C. Heiple, W. Bennett and T. Rising, "Embrittlement of ASTM Type XM-11 and AISI 304 and 430 Stainless Steels by Liquid Copper and Several Liquid Braze Alloys," Rockwell International, Rocky Flats Division, private communication.
8. H. B. Bott, "How to Weld Copper to Stainless Steel and Mild Steel," Welding Journal, 38, 236 (1959).

UNLIMITED RELEASE

DISTRIBUTION:

U. S. Department of Energy (171 for UC-71)
Technical Information Center
Oak Ridge, TN 37830

U. S. Department of Energy (7)
Energy Technology - Waste
Washington, D. C. 20545
Attn: R. B. Chitwood (5)
F. P. Falci
J. A. Sisler

U. S. Department of Energy
Albuquerque Operations Office
P. O. Box 5400
Albuquerque, NM 87185
Attn: E. C. Hardin

U. S. Nuclear Regulatory Commission (3)
Washington, D. C. 20555
Attn: D. R. Hopkins, MS NL5650
W. R. Lahs, Jr., MS 1130SS
C. E. McDonald, MS 396-SS

U. S. Department of Transportation
Materials Transportation Branch
Washington, D. C. 20590
Attn: Richard R. Rawl

Battelle Pacific Northwest Laboratory
P. O. Box 999
Richland, WA 99352
Attn: Russell E. Rhoads

Los Alamos Scientific Laboratory
P. O. Box 1663
Los Alamos, NM 87545
Attn: David Smith

Oak Ridge National Laboratory
P. O. Box X
Oak Ridge, TN 37830
Attn: L. B. Shappert

1500 W. A. Gardner
1530 W. E. Caldes
1535 D. C. Bickel
4400 A. W. Snyder
4410 D. J. McCloskey
4440 G. R. Otey
4442 W. A. Von Riesemann
4500 E. H. Beckner
4550 R. M. Jefferson
4551 R. E. Luna
4551 J. D. McClure
4552 R. B. Pope (25)
4552 H. R. Yoshimura (50)
4700 J. H. Scott
5500 O. E. Jones
5520 T. B. Lane
5800 R. S. Claassen
Attn: 5820 R. E. Whan
5840 H. J. Saxton
5830 M. J. Davis
Attn: 5831 N. J. Magnani
5832 R. W. Rohde
5833 J. L. Jellison
5836 J. L. Ledman
5832 T. J. Lutz
5832 J. W. Munford
5833 G. Knorovsky
5835 C. H. Karnes
5835 H. J. Rack (4)
5835 J. A. Van Den Avyle
5835 M. S. Soo Hoo
5835 R. E. Blose
5835 W. B. Jones
8266 E. A. Aas
3141 T. L. Werner (5)
3151 W. L. Garner (3)
For DOE/TIC (Std. distr. UC-71)
4551 TTC Library (5)
File Ref. 3003.032